Monte-Carlo Simulation of Multisite Echinomycin–DNA Interactions Detected by in Vitro Transcription Analysis†

Don R. Phillips,*,‡ Robin J. White,‡ David Dean,§ and Donald M. Crothers§

Biochemistry Department, La Trobe University, Bundoora, Victoria 3083, Australia, and Department of Chemistry, Yale University, New Haven, Connecticut 06511

Received November 28, 1989

ABSTRACT: The interaction of echinomycin with DNA was analyzed at 37 °C by in vitro transcription analysis using a 497 bp fragment of DNA containing the *lac* UV5 promoter. Sixteen discrete drug binding sites were detected. The mole fraction of blocked transcript at each site was monitored over 4 h, and the kinetic profile was analyzed by Monte-Carlo simulation. The time course for all 16 sites was fully described by this process. For each drug site, three parameters were resolved with the following variation between sites: relative drug occupancy (1–26), dissociation rate constant (0.06–0.70 min^{-1}), and probability of termination of transcription (0–48%). Eight low-occupancy binding sites were at 5′-CA sequences (relative occupancy of 1.0–2.9). The eight major sites were all at 5′-CG sequences (relative occupancy of 6.3–26) and exhibited an average occupancy some 13-fold greater than the CA sites, corresponding to an average additional stability of approximately 1.6 kcal. The dissociation rates from apparent high-affinity sites were only partially correlated with relative occupancy. Ten binding sites exhibited a 3–48% probability of termination of transcription immediately adjacent to the 5′-CG central sequence. Termination probably arises from distortion of the DNA helix in regions flanking the binding site and was most dramatic (48% probability) where two adjacent CG sites were separated by only 1 bp. This termination phenomenon may well account for the observed effects of echinomycin in vivo.

As a result of correlations that have been made between DNA binding and the action of anticancer drugs, the question has arisen as to whether this effect is due to the thermodynamic affinity of the drug for DNA or to the kinetics of dissociation of drug from the DNA (Siegfried et al., 1983; Ralph et al., 1983; Wilson & Jones, 1981; Brown, 1978).

There is good evidence to support the notion of affinity being the dominant factor, as illustrated by the correlation of DNA binding affinity of anthracycline derivatives (over 3 orders of magnitude), with their biological activity (Valentini et al., 1985). There is also an increasing amount of evidence in support of the concept that the dissociation kinetics may be an important determinant of anticancer activity (Müller & Crothers, 1968; Gabbay et al., 1976; Wilson et al., 1976; Aktipis & Panayotatos, 1981; Wakelin & Waring, 1980; Fox & Waring, 1981; Waring & Fox, 1983; Feigon et al., 1984; Denny et al., 1985; Fox et al., 1985; Gandecha et al., 1985; Wakelin et al., 1987).

If the drug–DNA dissociation kinetics are indeed an important aspect of biological activity of the drug, it becomes critical to establish which biological or physicochemical procedures yield meaningful values for the dissociation process. The most rigorous physicochemical procedures for analysis of drug–DNA kinetics involve T-jump or stopped-flow relaxation methods (Bernasconi, 1976; Chaires et al., 1985) but are exceedingly tedious and time-consuming. A more rapid procedure which yields just the dissociation kinetic parameters is a detergent sequestering technique introduced by Müller and Crothers (1968), and widely employed since then for a variety of DNA binding drugs (Chaires et al., 1985; Wakelin, 1986). This procedure relies on an essentially unidirectional sequestration of drug by SDS micelles, with the drug kinetics being monitored by a change of absorbance accompanying the process in going from bound to free drug. While this technique provides an extremely rapid means of quantifying drug–DNA dissociation kinetics, it is complicated by the contribution to the kinetic parameters by the forward reaction(s), and by possible effects of the detergent on the stability of the drug–DNA complex. However, the major limitation of this approach is that the dissociation of drugs from "random-sequence" DNA gives rise to multiple dissociation exponentials due to site microheterogeneity (Krugh et al., 1980). The analysis of such data is in terms of a multiexponential fit, which represents an averaging of binding sites within various resolvable kinetic processes (Phillips et al., 1988). The alternative approach is to examine the dissociation kinetics using homopolymers such as poly(dG·dC) which yield single-exponential dissociation curves (Fox & Waring, 1984), but this fails to yield an unambiguous representation of drug action in vivo, where flanking sequences could have a major contribution to the drug–DNA interaction. Indeed, the influence of flanking sequences immediately adjacent to the actinomycin D intercalation sites has been recently documented (Chen, 1988a,b).

A new procedure has recently been established to yield drug–DNA dissociation kinetics under conditions of active transcription of the DNA (Phillips & Crothers, 1986; White & Phillips, 1988). This procedure yields a physiologically more meaningful measure of dissociation kinetics than the physicochemical procedures outlined above. A surprising result obtained from this transcription assay was that the time constant for dissociation of drug from the DNA (i.e., residence time) was longer as measured by the transcription assay than by detergent sequestration (Phillips & Crothers, 1986). This was unexpected since transcription involves opening of the DNA adjacent to the drug binding site, with a potential concomitant destabilization of the drug–DNA complex. A possible explanation for these observations is that in the de-

† This work was supported by the Australian Research Committee.

‡ La Trobe University.

§ Yale University.

0006-2960/90/0429-4812$02.50/0

tergent sequestering procedure an average value is measured, reflecting dissociation from a range of drug binding sites. This averaged value must be compared with that detected by the transcription assay, where dissociation from a single defined site is measured. The implication of this interpretation is that the range of dissociation time constants would also be detected by the transcription assay if a sufficient number of binding sites were probed at appropriate drug loadings. For this reason, an analysis of the dissociation kinetics of a range of drug sites was probed by transcription footprinting in order to detect the heterogeneity of affinity and dissociation parameters at each individual drug binding site, and also to assess the effect of flanking sequences on these parameters. Echinomycin was used as a model drug for this work since it exhibited dissociation characteristics which were similar to those of actinomycin D (White & Phillips, 1988) and therefore enabled convenient sampling times commensurate with experimental limitations of the transcription assay.

Quantitation of multiple drug–DNA dissociation parameters derived from in vitro transcription studies is complex because of the effect of read-through of RNA polymerase from one drug site to the next (White & Phillips, 1988). The kinetic parameters derived from a previous study of multiple actinomycin D binding sites on DNA were approximations, based on minimal read-through resulting from a unique delayed termination accompanying several of the sites (White & Phillips, 1988). For the present work, a more rigorous approach was required in order to yield meaningful kinetic parameter devoid of such approximations. The procedure chosen was a Monte-Carlo simulation analysis. We present here a general method for the simulation analysis of multiple ligand–DNA interactions and show that it can be successfully applied to solve for up to 48 parameters describing 16 discrete drug binding sites on DNA.

Materials and Methods

Materials. Echinomycin was provided by Dr. L. P. G. Wakelin, Cancer Institute, Melbourne. A 497 bp DNA fragment containing the *lac* UV5 promoter was isolated as described previously (White & Phillips, 1988). All other materials were as described previously (White & Phillips, 1988).

Transcription Assay. The in vitro transcription assay, electrophoresis of transcripts, and RNA sequencing procedure were all as described previously (White & Phillips, 1988). Echinomycin (12 μM) was equilibrated with the initiated complex at 37 °C for 30 min, and then elongation was commenced by the addition of high levels of all four nucleotides (to 2.5 mM) in 400 mM KCl. These conditions minimized natural pausing which would otherwise complicate interpretation of drug-induced effects.

Quantitation of RNA Transcripts. Autoradiograms were scanned by using a Biomed Model SL-504-XL laser densitometer linked to a Spectra Physics SP4270 integrator. Every band was scanned 5 times and the average area used for further quantitation. The standard error of these replicates for each band varied from 10 to 30%, but was ±10% for most. Each lane was normalized with respect to the total amount of radioactivity, and echinomycin-induced pauses were calculated as a percentage of this total radioactivity. Since radiolabel was incorporated only into the initiated 10-mer (label was diluted extensively in the elongation phase), each RNA transcript contained the same amount of radiolabel—the normalized amount of each band within each lane therefore represents the mole fraction of blocked transcript.

Monte-Carlo Simulation. A FORTRAN program (SIMULA) was developed to simulate the time course for movement of RNA polymerase along the DNA. The DNA was represented as an array, with one element for each drug site. Each element was cleared (no drug bound) or set to a nonzero value. A counter was used to mark the polymerase position at any point of time. At each iteration, any occupied drug site in a given molecule can become freed, with a probability equal to the product of the time interval (δt) and the dissociation rate constant (k_d) for that site—the polymerase will then advance to the next occupied site, or proceed to yield the full-length transcript. The time interval used routinely was 0.01 min and was selected as a balance between a smaller interval (with increased computer processing time) and decreased resolution of the simulation at larger time intervals. The program therefore checks for drug dissociation at each pass and updates the RNA polymerase position on each DNA molecule. Termination of transcription at individual drug sites was allowed for by assigning a rate constant for dissociation of RNA polymerase from the transcription complex at each site (k_t). Since the rate of termination competes with the rate of read-through to the next site (defined by k_d), the integrated probability of termination at each site is therefore given by $k_t/(k_t + k_d)$.

The program used an ensemble of 100000 DNA molecules, represented by a two-dimensional array, with drug sites filled by random assignment. The algorithm assumes that RNA polymerase does not pause or terminate at empty sites, and moves rapidly from one site to the next, compared to the rate of drug dissociation. This is a reasonable approximation given that under optimal conditions RNA polymerase transcribes 30–60 nucleotides per second (von Hippel et al., 1984). The first round of simulation used values obtained by fitting the experimentally derived data to an exponential function. The values for drug occupancy, dissociation rate, and termination rate were then varied until the decay of transcripts at the first drug site was fitted to the observed values. All other drug sites were fitted in succession in the same manner.

The simulation procedure was therefore used to generate initial drug occupancy, a drug dissociation rate constant, and a termination rate constant for each site, as well as statistical estimates of the fit.

Results

Transcription Assay. The transcription assay relies upon the formation of a stable initiation complex with the RNA of all transcripts synchronized to known lengths. This was achieved by forcing transcription to begin selectively from one start site in the promoter region (with high levels of GpA, complementary to the −1 and +1 positions of the UV5 promoter) and allowing transcription to proceed up to a nucleotide missing from the transcription mixture (Phillips & Crothers, 1986; White & Phillips, 1988). For the UV5 promoter, the absence of CTP yields RNA comprising mainly 10-mers, and small amounts of 17- and 23-mers (Figure 1 and Figure 2, lane I). This read-through has been noted previously and is thought to be due either to misincorporation of other nucleotides or to trace levels of contaminating CTP (Carpousis & Gralla, 1985; White & Phillips, 1988). Addition of the missing CTP enables elongation to proceed to a full-length transcript within 1 min, with only minor degradation (probably by RNase) after 230 min (Figure 1).

Effect of Echinomycin. When echinomycin was equilibrated with the initiated transcription complex, and then CTP added to enable elongation to occur, a range of discrete length transcripts was observed (Figure 2). Although most of the drug-induced blockages decayed with time, resulting in a

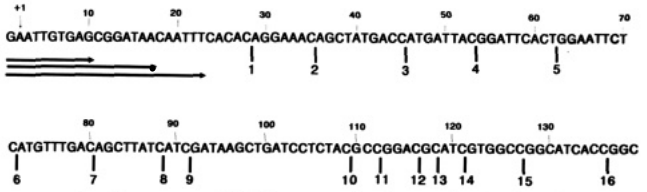

FIGURE 1: Sequence of UV5 transcript from the 497 bp fragment of pRW1. Initiation was GpA from the −1 and +1 positions. Transcript lengths are numbered from the first residue of the RNA (i.e., from the −1 position). The three major initiation transcripts (10-, 17-, and 23-mers) are shown by arrows below the sequence. The location of all echinomycin-induced blocked transcripts has been shown and numbered from 1 to 16.

concomitant build-up of full-length transcript, many exhibited limited read-through even after 4 h following commencement of elongation (Figure 2).

The mole fraction of each transcript was calculated from the relative intensity of each band within each lane. Sixteen transcripts were resolved (Figure 2), and a time course for the profile of the mole fraction of each blocked transcript is shown in Figures 3 and 4.

For each drug-induced blocked transcript, the three parameters describing each drug site (initial occupancy, drug dissociation rate constant, and rate constant for the dissociation of RNA polymerase from the transcription complex) were evaluated, and the predicted profile for the amount of RNA polymerase at each drug site is shown as a continuous line in Figures 3 and 4. The experimental values for all drug sites are adequately described by the simulated profiles except for site 10, where all experimental values for $t > 20$ min were overestimated (and not fitted) because the full-length transcript was outside the range of photographic linearity, and was therefore underestimated for latter time points.

The dashed lines in Figures 3 and 4 show the actual drug occupancy at each site. This curve completely overlaps the profile for the calculated amount of RNA polymerase retarded at the first drug site, but for subsequent sites, an increasing difference is observed between these two values. This arises because downstream sites become increasingly hidden behind occupied drug sites the further transcription proceeds (White & Phillips, 1989a,b).

The parameters employed in the simulation (Figures 3 and 4) are summarized in Table I, and the location of the 16 echinomycin sites in the transcribed sequence is shown in

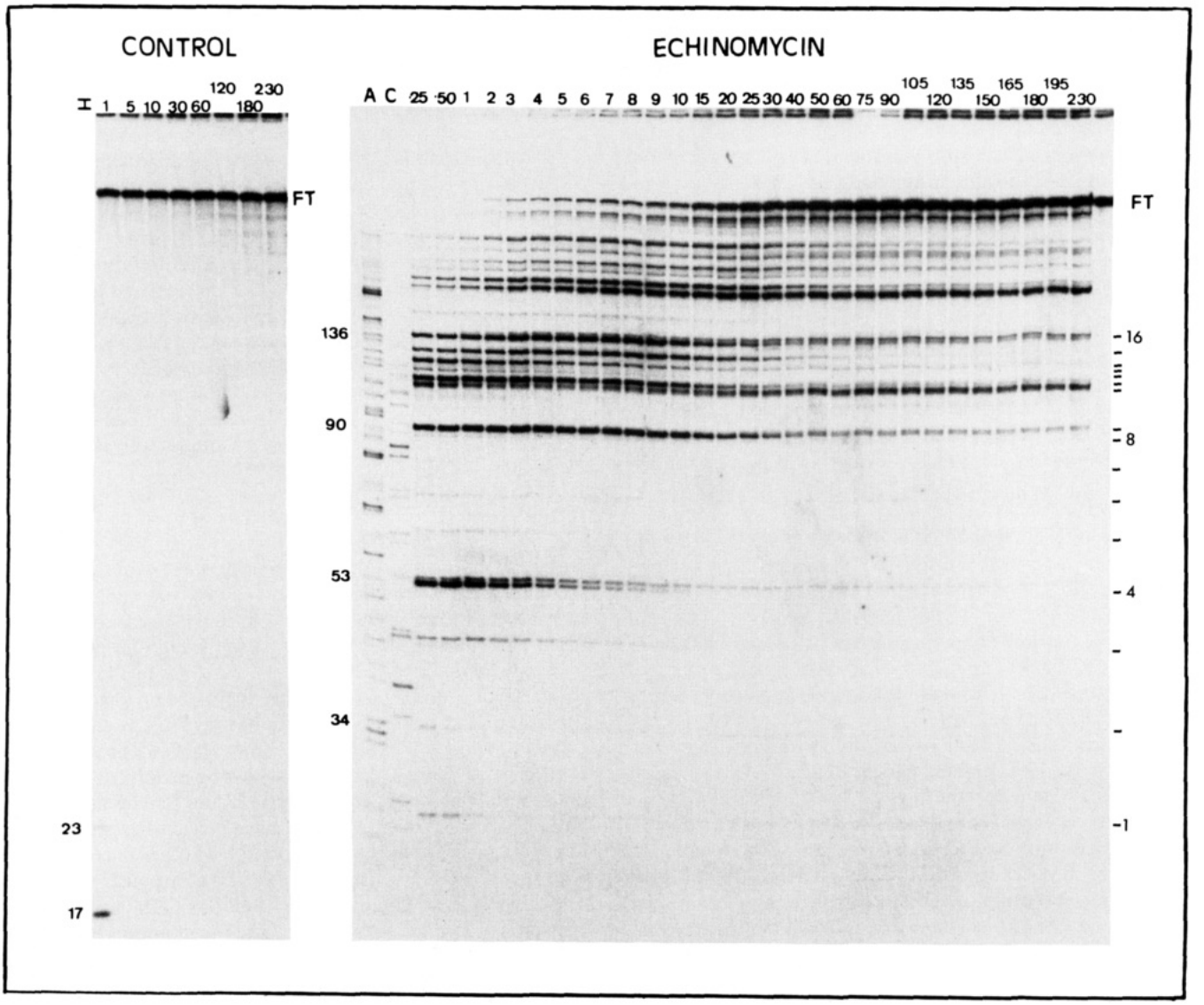

FIGURE 2: Autoradiogram of multiple echinomycin-induced blocked transcripts. The initiated complex is shown in lane 1, and also after incubation with echinomycin for 30 min and elongation for 0.25–230 min. Drug-induced blocked transcripts which were subjected to simulation analysis are numbered 1–16. The control lanes show the transcripts observed 1–230 min after elongation in the absence of echinomycin. The full-length transcript (380 residues) is denoted as FT. Sequencing lanes A and C represent elongation of the initiated complex in the presence of 3′-*O*-methyl-ATP and 3′-*O*-methyl-CTP, respectively (White & Phillips, 1989a,b).

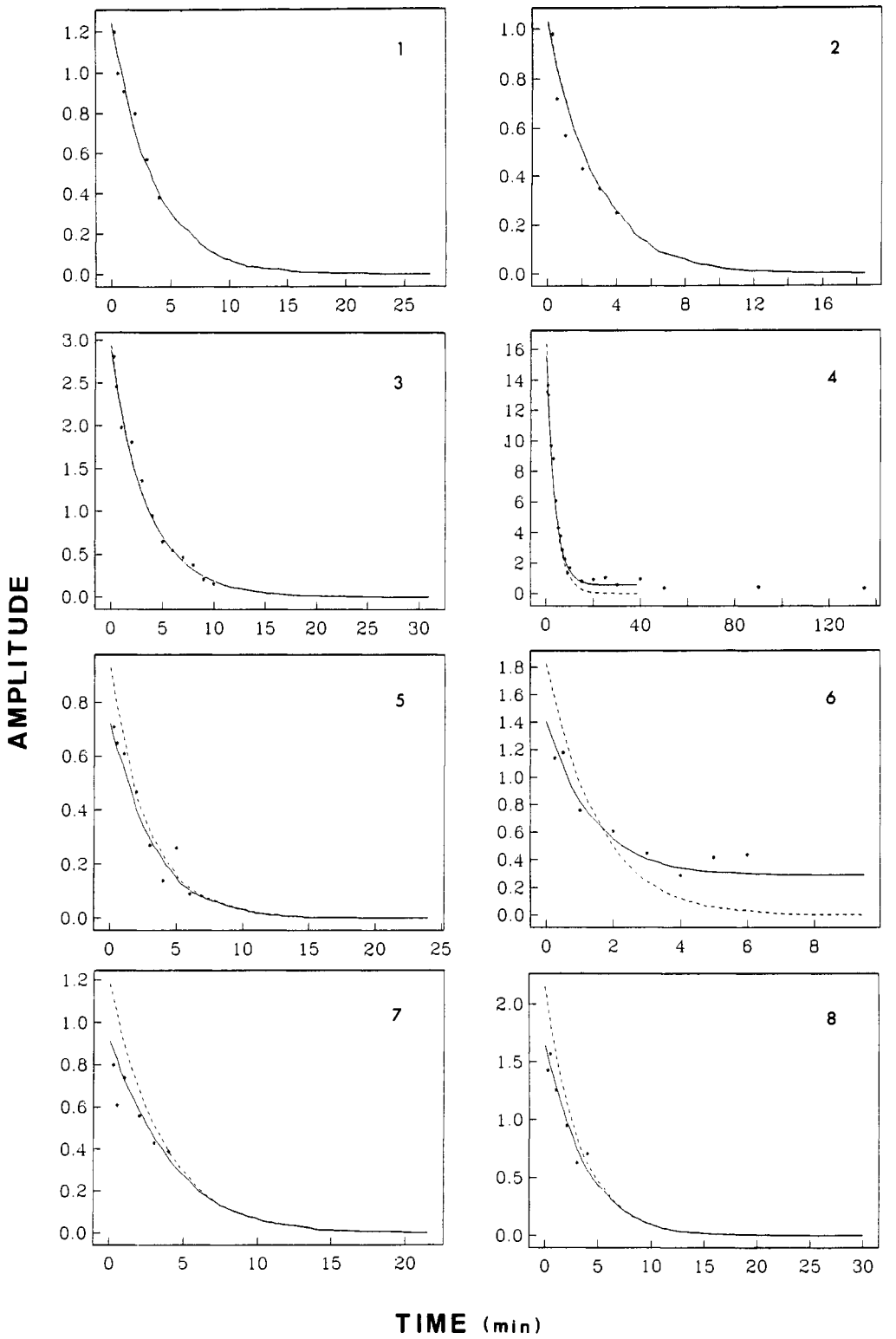

FIGURE 3: Simulation analysis of echinomycin-induced blocked transcripts, drug sites 1–8. The autoradiogram (Figure 2) was subjected to quantitative analysis 5 times, and the average mole fraction (as a percentage) of blocked transcripts is shown by asterisks as a function of elongation time. The simulated amount of blocked transcripts is shown as a continuous line, and the calculated drug occupancy at each site is represented by a dashed line.

Figure 1. Eight of the blocked transcripts occurred prior to a 5′-CA sequence (Table I), and these were all associated with low drug occupancy (≤2.9). The other eight blocked transcripts were all prior to 5′-CG sequences, and all exhibited high drug occupancies (≤16.3).

Discussion

Validity of the Simulation. For each drug site, the rate of change of blocked transcript has three components—the rate of dissociation of drug from that site (k_d), the extent of read-through of RNA polymerase from all upstream sites, and the termination rate (k_t). Thus, once the occupancy and k_d have been evaluated for decay from the first site (a simple first-order process), all subsequent k_d values can then be estimated.

The initial drug occupancy is defined by the extrapolated occupancy at zero time. A good estimate of this parameter is therefore required to enable an adequate fit to the observed

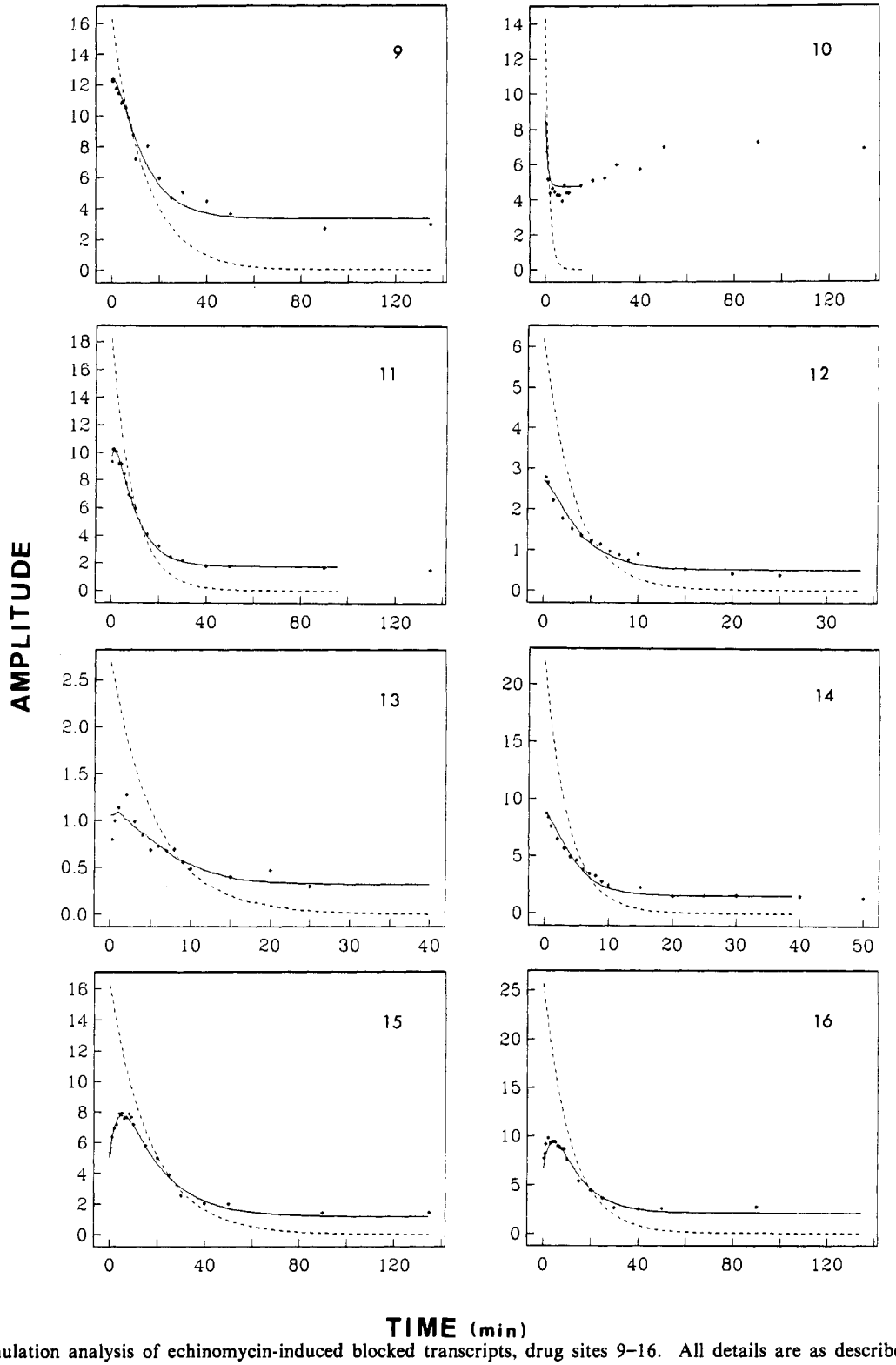

FIGURE 4: Simulation analysis of echinomycin-induced blocked transcripts, drug sites 9–16. All details are as described for Figure 3.

levels of blocked transcript as a function of time.

Once the initial drug occupancy has been solved, it is a simple matter to estimate k_t, since the fractional probability of termination is given by $k_t/(k_t + k_d)$, and is related to the experimental data by the ratio of the amount of transcript at infinite time compared to the initial drug occupancy. If a reproducible set of experimental values is available for the apparent occupancy at infinite time (e.g., Figure 4, sites 14 and 16), then k_t can be estimated with confidence. In other cases where only limited time-independent data are available (e.g., Figure 4, site 15), any such estimate of k_t must be treated with obvious caution.

Although the three parameters describing each drug site are not independent of each other, three different aspects of the experimental decay curve must be fitted, and this enables a unique best-fit solution to be achieved for each drug site. Clearly, other solutions are possible, but these arise only because of the variation inherent within the experimental data set. The most rigorous data set would require for each drug site at least three data points close to zero time, at least six data points describing the decay, and a further three time-independent values. Since the decay zone will be observed at considerably different times for different drug sites (0–5 min in Figure 3, site 1, compared to 10–40 min in Figure 4, site

Table I: Simulation Parameters Used To Fit the Experimental Transcription Data (Figures 3 and 4) for the Binding of Echinomycin to DNA

site	sequence	relative occupancy	dissociation rate constant (min^{-1})	termination rate constant	
				min^{-1}	%
1	ACAG	1.25	0.29		
2	ACAG	1.00	0.37		
3	CCAT	3.00	0.28		
4	ACGG	16.40	0.27	0.009	3
5	CTGG	1.00	0.36		
6	TCAT	1.88	0.65	0.16	20
7	ACAG	1.20	0.27		
8	TCAT	2.21	0.30		
9	TCGA	16.2	0.07	0.019	21
10	ACGC	14.4	0.65	0.59	48
11	CCGG	18.5	0.11	0.016	13
12	ACGC	6.27	0.31	0.047	13
13	GCAT	2.90	0.20	0.045	18
14	TCGT	22.0	0.27	0.037	12
15	CCGG	16.2	0.058	0.0063	10
16	CCGC	25.7	0.086	0.013	13

15), depending on the drug dissociation rate at that site and its location relative to other sites, an extended sampling time is required to enable the best simulation to be achieved. The 10-fold time range illustrated in Figure 3 (site 1) and Figure 4 (site 14) for accumulation of data therefore implies a minimum of 96 sampling times if the ultimate experimental data set is to be obtained in this situation. This is not practical, and the lesser number of sampling times which can be analyzed reliably on a single electrophoresis gel then becomes one of the constraints of this approach.

All three parameters for every upstream site influence the simulated amount of RNA polymerase able to reach downstream sites. The fact that the simulation enables the appropriate amount of read-through of RNA polymerase to latter sites (e.g., sites 15 and 16, Figure 4) indicates that the parameters for earlier sites are adequate, since they must also describe the buildup of blocked transcripts at early time points for the latter sites. As shown in Figure 4, sites 15 and 16, the good fit of the early time points provides an additional test of the validity of the parameters describing previous drug sites.

Relative Drug Occupancy. The values for relative occupancy of echinomycin at each site were derived from the mole fraction (as a percentage) of RNA at zero elongation time. At early time points, transcription proceeds to the first drug-occupied site, and later occupied drug sites are not observed (Figure 5). There is therefore an increasing differential between observed blocked transcript and actual drug occupancy, the further transcription proceeds. The simulation analysis overcame this problem of quantitation since it is based on fitting of the calculated amount of blocked transcript (based on actual drug occupancy at each site) to the observed values. For this reason, all values for occupancy shown in Table I are *relative* to the observed occupancy at this first drug site.

An earlier method to estimate actual drug occupancy from relative amounts of blocked transcripts utilized the statistical probability that downstream drug sites lie behind occupied upstream sites (White & Phillips, 1989a,b). While this procedure provides a simple means of approximating drug occupancy from transcription data, it does not take any account of read-through of RNA polymerase from one drug-occupied site to the next. This procedure will therefore only be valid for drugs with a long half-life, and at early sampling times. The method of simulation analysis has no such constraints and is a general procedure for the quantitative analysis of any transcription-derived data from any site-specific ligand–DNA interacting system.

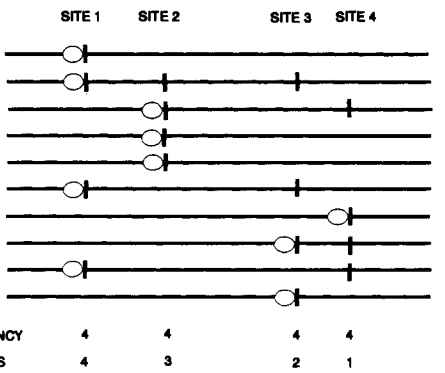

FIGURE 5: Diagrammatic representation of drug occupancy and blocked transcripts. Four drug binding sites are shown on 10 DNA molecules, with an equal probability of occupancy at each site. The location of RNA polymerase is shown immediately after commencement of the elongation phase. For the first drug site, occupancy will be reflected by a blocked transcript. However, for later drug sites, there is an increasing probability that an occupied site will lie behind an occupied earlier site, and therefore not be detected.

Sequence Specificity. Echinomycin is known to bisintercalate into DNA, adopting a staplelike conformation centered about 5′-CG base pairs, with the cyclic octapeptide linker protruding into the minor groove, with many specific hydrogen bond and van der Waals contacts between the peptides and the DNA (Wakelin, 1986; Waring, 1987). Both crystal X-ray diffraction and NMR studies have shown that the "sandwiched" CG base pairs adopt Watson–Crick pairing, while T on the 5′ side flanking the intercalation site adopts Hoogesteen pairing in short oligonucleotides (Wang et al., 1987; Quigley et al., 1986; Gao & Patel, 1988).

The observation that all high-occupancy sites are 5′-CG sequences is as expected, based on the detailed DNase I and MPE-Fe(II) footprinting studies of Low et al. (1984) and Van Dyke and Dervan (1984), respectively. Since all other low-occupancy sites were at 5′-CA sequences, it must be concluded that the only two preferred sequences are CG and CA, with the latter exhibiting, on average, a 13-fold lower occupancy. The echinomycin–CG complexes are therefore an average of 1.6 kcal more stable than the echinomycin–CA complex, and this suggests the presence of one or more additional stabilizing contacts in the former complex (Andrews et al., 1984). This quantitative analysis is also consistent with a comparison of structural differences from crystal X-ray diffraction studies, where the substitution of G with A would be expected to result in the loss of one hydrogen bond between the alanine residue of echinomycin and the G residue of DNA, with no loss of van der Waals contacts (Wang et al., 1984; Ughetto et al., 1985).

No flanking sequence specificity was apparent for nucleotides 3′ to the central 5′-CG site, since for the four highest occupancy sites all four nucleotides were represented. However, for the same four sites, only C and T occur on the 5′ side. The preference for T on the 5′ side has also previously been observed by MPE-Fe(II) footprinting (Van Dyke & Dervan, 1984), and this may relate to the known Hoogsteen pairing of this base pair (Wang et al., 1984; Quigley et al., 1986; Gao & Patel, 1988).

The binding site size for echinomycin has previously been determined as 4 bp by chemical footprinting (Van Dyke & Dervan, 1984) and 6 bp by nuclease footprinting (Low et al., 1984). The 2-fold variation of occupancy observed between ACGC sites 10 and 12, and the 2-fold variation of drug dissociation rate between CCGG sites 11 and 15 (Table I), provides strong support for the notion that sequences flanking

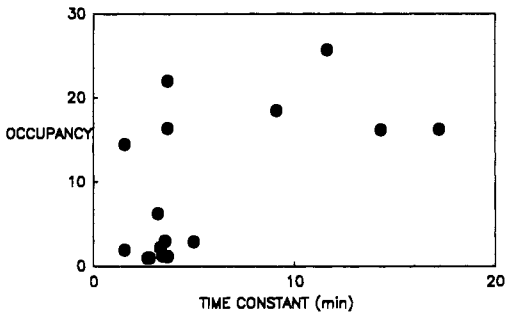

FIGURE 6: Relationship between relative drug occupancy and drug time constant ($1/k_d$). The simulation-derived parameters (Table I) are shown for each echinomycin site.

the tetranucleotide binding site are also important determinants of the interaction. This has also been indicated by enhanced nuclease susceptibility in dominantly A·T regions flanking echinomycin binding sites (Low et al., 1984), which suggests an altered helix structure in these regions. The fact that RNA polymerase reads right up to the base pair of the echinomycin intercalation site confirms the view that the cyclic peptide linker protrudes into the minor groove (Waring, 1987), given that the polymerase tracks in the major groove (White & Phillips, 1988).

Drug Dissociation Rates. If the interaction of echinomycin with each site is described by a simple equilibrium process, then the occupancy (a measure of binding affinity) would be inversely related to the rate of dissociation from each site, assuming the association rates to be independent of DNA sequence. The scatter of points in Figure 6 shows that only a general correlation exists. While the errors associated with quantitation of blocked transcripts (±15–30%) and reproducibility of the simulation (±10%) account for some of the variation, it is probable that sequence-dependent effects of the transcription complex, or of the termination process, will influence the apparent occupancy or apparent dissociation rate, but we have not been able to document such events from the present simulation. Irrespective of these factors, there is a general trend that the higher the occupancy, the smaller the dissociation rate.

Detergent-sequestered dissociation of echinomycin from calf thymus DNA has been resolved as comprising three exponential components with time constants of 5.8, 19, and 155 s (I = 0.1, 20 °C) with corresponding amplitudes of 47, 47, and 6% (Fox et al., 1981). These time constants span a 27-fold range, comparable to the 15-fold range observed at the limited number of individual sites probed by RNA polymerase (Table I). The wide range of dissociation rates detected by the transcription assay therefore provides direct support for the view that kinetic parameters derived from detergent sequestration reflect the number of resolvable components, each of which is an average of a range of values from individual sites (Fox et al., 1981). This interpretation has also been confirmed recently with the anthracycline antibiotics (Phillips et al., 1988).

The slowest transcription-detected dissociated rate was at site 15 (k_d = 0.055 min^{-1}; time constant = 1090 s), some 7-fold slower than observed by detergent sequestration under similar conditions (Fox et al., 1981). This apparent enhanced drug residence time on DNA under transcription conditions (compared to physicochemical methods) has also been noted with actinomycin D, and is thought to be due to a cage effect of the RNA polymerase in restricting the solution volume accessible to free drug (White & Phillips, 1989c).

Probability of Termination. Although small amounts of termination of transcription have been noted at drug binding sites (Flamée, 1985; White & Phillips, 1988), they have not previously been quantitated. There are three major possible causes of the observed termination of transcription at echinomycin binding sites. A simple hypothesis is that the termination arises from destabilization by a RNA hairpin helix within the 30 bp spanned by the open transcription complex—a careful computer analysis of all possible hairpins revealed that for these sites which exhibited termination, only half are located appropriately downstream of potential hairpin-forming regions. A second explanation is that regions immediately downstream of the binding sites provide critical destabilization features; however, no such features are readily apparent. The third and most likely explanation is that the mere delay of transcription induced by the presence of echinomycin, together with the local changes of DNA secondary structure accompanying the extensive unwinding of DNA (44–50°) that occurs upon bisintercalation of this drug (Waring & Fox, 1983), is sufficient to destabilize the ternary complex. On the basis of the average of 17% probability of termination at 10 sites, the half-life of the ternary transcription complex is approximately 10 min, compared to many hours in the absence of echinomycin, as shown by the control lanes in Figure 2. If this view is correct, then some termination would be expected to be observed at every echinomycin site since the drug off-rates differ by only 1 order of magnitude. This may well prove to be correct, since the only sites where termination was not observed were low-occupancy sites (1–3, 5, 7, and 8) where there was insufficient data to indicate either the presence or the absence of the termination phenomenon.

With regard to the termination process, it is interesting to note that transcription by bacteriophage RNA polymerase is also terminated at drug binding sites (White & Phillips, 1989a). A similar process may also occur with bacterial transcription systems—given their additional complexity, it would not be unexpected if more complex features emerged, such as modulation by altered DNA secondary structures and other, as yet unknown, effects.

Site 10 is unique because of the high probability of termination at this ACGC sequence. The tetrameric sequence itself is not a critical determinant of termination—it is repeated at site 12 which does not exhibit unusual termination compared to sites 4, 9, 11, and 14–16. The high termination probability of site 10 probably derives from the accumulative perturbed DNA secondary structure associated with the two adjacent high-affinity sites 10 and 11, separated by only 1 bp (Figure 1).

Implications for Drug–DNA Interactions. Many of the known DNA-acting clinically active drugs are intercalators (Gale et al., 1981; Waring, 1981, 1987). It has generally been assumed that these compounds act by inhibiting the rate of progression of either DNA polymerase and/or RNA polymerase along the template, thereby inhibiting the rate of DNA replication or transcription (Wilson & Jones, 1981). It is difficult to see why the mere *delay* of the rate of DNA or RNA synthesis would be so cytotoxic, and it is now apparent that a more lethal process, that of *termination* of transcription at individual drug sites, provides a more plausible mechanism of action of these intercalating drugs. Proof of this model awaits the analysis of blocked transcripts in vivo, and these studies are currently in progress.

ACKNOWLEDGMENTS

We thank Dr. L. P. G. Wakelin, Cancer Institute, Melbourne, for the gift of echinomycin and Vicki Kurrle for the simulation analyses.

References

Aktipis, S., & Panayotatos, N. (1981) *Biochim. Biophys. Acta 655*, 278–290.

Andrews, P. R., Craik, D. J., & Martin, J. L. (1984) *J. Med. Chem. 27*, 1648–1657.

Bernasconi, C. F. (1976) *Relaxation Kinetics*, Academic Press, New York.

Brown, J. R. (1978) *Prog. Med. Chem. 15*, 125–164.

Carpousis, A. J., & Gralla, J. D. (1985) *J. Mol. Biol. 183*, 165–177.

Chaires, J. B., Dattagupta, N., & Crothers, D. M. (1985) *Biochemistry 24*, 260–267.

Chen, F. (1988a) *Biochemistry 27*, 1843–1848.

Chen, F. (1988b) *Biochemistry 27*, 6393–6397.

Denny, W. A., Atwell, G. J., Baguley, B. C., & Wakelin, L. P. G. (1985) *J. Med. Chem. 28*, 1568–1574.

Feigon, J., Denny, W. A., Leupin, W., & Kearns, D. R. (1984) *J. Med. Chem. 27*, 450–465.

Flamée, P.-A. (1985) *Biochem. J. 230*, 557–560.

Fox, K. R., & Waring, M. J. (1981) *Biochim. Biophys. Acta 654*, 279–286.

Fox, K. R., & Waring, M. J. (1984) *Eur. J. Biochem. 145*, 579–586.

Fox, K. R., Wakelin, P. G., & Waring, M. J. (1981) *Biochemistry 20*, 5768–5779.

Fox, K. R., Brassett, C., & Waring, M. J. (1985) *Biochim. Biophys. Acta 840*, 383–392.

Gabbay, E. J., Grier, D., Fingerle, R. E., Reimer, R., Levy, R., Pearce, S. W., & Wilson, W. D. (1976) *Biochemistry 15*, 2062–2070.

Gale, E. F., Cundliffe, E., Reynolds, P. E., Richmond, M. H., & Waring, M. J. (1981) *The Molecular Basis of Antibiotics Action*, 2nd ed., Wiley, London.

Gandecha, B. M., Brown, J. R., & Crampton, M. R. (1985) *Biochem. Pharmacol. 34*, 733–736.

Gao, X., & Patel, D. J. (1988) *Biochemistry 27*, 1744–1751.

Krugh, T. R., Hook, J. W., & Balakrishnan, M. S. (1980) in *Nucleic Acid Geometry and Dynamics* (Sarma, R. H., Ed.) pp 351–366, Permagon, New York.

Low, M. L., Drew, H. R., & Waring, M. J. (1984) *Nucleic Acids Res. 12*, 4865–4879.

Müller, W., & Crothers, D. M. (1968) *J. Mol. Biol. 35*, 251–290.

Phillips, D. R., & Crothers, D. M. (1986) *Biochemistry 25*, 7355–7362.

Phillips, D. R., Greif, P. C., & Boston, R. C. (1988) *Mol. Pharmacol. 33*, 225–230.

Quigley, G. J., Ughetto, G., van der Marel, G. A., van Boom, J. H., Wang, A. H.-J., & Rich, A. (1986) *Science 232*, 1255–1258.

Ralph, R. K., Marshall, B., & Darkin, S. (1983) *Trends Biochem. Sci. (Pers. Ed.) 8*, 212–214.

Siegfried, J. M., Sartorelli, A. C., & Tritton, T. R. (1983) *Cancer Biochem. Biophys. 6*, 137–142.

Ughetto, G., Wang, H.-J., Quigley, G. J., van der Marel, G. A., van Boom, J. H., & Rich, A. (1985) *Nucleic Acids Res. 13*, 2305–2323.

Valentini, L., Nicolella, V., Vannini, E., Menozzi, M., Penco, S., & Arcamone, F. (1985) *Farmaco, Ed. Sci. 40*, 376–390.

Van Dyke, M. W., & Dervan, P. B. (1983) *Biochemistry 22*, 2373–2377.

Van Dyke, M. W., & Dervan, P. B. (1984) *Science 225*, 1122–1127.

von Hippel, P. H., Bear, D. G., Morgan, W. D., & McSwiggen, J. A. (1984) *Annu. Rev. Biochem. 53*, 389–446.

Wakelin, L. P. G. (1986) *Med. Res. Rev. 6*, 275–340.

Wakelin, L. P. G., & Waring, M. J. (1980) *J. Mol. Biol. 144*, 183–214.

Wakelin, L. P. G., Atwell, G. J., Rewcastle, G. W., & Denny, W. A. (1987) *J. Med. Chem. 30*, 855–861.

Wang, A. H., Ughetto, G., Quigley, G. J., & Rich, A. (1987) *Biochemistry 26*, 1152–1163.

Waring, M. J. (1981) *Annu. Rev. Biochem. 50*, 159–192.

Waring, M. J. (1987) in *DNA–Ligand Interactions. From Drugs to Proteins* (Guschlbauer, W., & Saenger, W., Eds.) pp 113–126, Plenum Press, New York.

Waring, M. J., & Fox, K. R. (1983) in *Molecular Aspects of Anticancer Drug Action* (Neidle, S., & Waring, M. J., Eds.) pp 127–156, Macmillan, London.

White, R. J., & Phillips, D. R. (1988) *Biochemistry 27*, 9122–9132.

White, R. J., & Phillips, D. R. (1989a) *Biochemistry 28*, 4277–4283.

White, R. J., & Phillips, D. R. (1989b) *Biochemistry 28*, 6259–6269.

White, R. J., & Phillips, D. R. (1989c) *Biochem. Pharmacol. 38*, 331–334.

Wilson, D. W., & Jones, R. L. (1981) *Adv. Pharmacol. Chemother. 18*, 177–222.

Wilson, D. W., Grier, D., Reimer, R., Bauman, J. D., Preston, J. F., & Gabbay, E. J. (1976) *J. Med. Chem. 19*, 381–384.